

Unraveling C4 selectivity in the light-driven C–H fluoroalkylation of pyridines and quinolines

Leejae Kim^{§1,2}, Wooseok Lee^{§1,2} and Sungwoo Hong^{*2,1}

¹Department of Chemistry, Korea Advanced Institute of Science and Technology (KAIST), Daejeon 34141, Korea

²Center for Catalytic Hydrocarbon Functionalizations, Institute for Basic Science (IBS), Daejeon 34141, Korea

Supporting Information Placeholder

ABSTRACT: Given the prevalence of pyridine motifs in FDA-approved drugs, selective fluoroalkylation of pyridines and quinolines is essential for preparing diverse bioisosteres. However, conventional Minisci reactions often face challenges in achieving precise regioselectivity due to competing reaction sites of pyridine and the limited availability of fluoroalkyl radical sources. Herein, we present a light-driven, C4-selective fluoroalkylation of azines utilizing *N*-aminopyridinium salts and readily available sulfinates. Our approach employs electron donor-acceptor complexes, achieving highly C4-selective fluoroalkylation under mild conditions without an external photocatalyst. This practical method not only enables the installation of CF₂H groups but also allows for the incorporation of CF₂-alkyl groups with diverse functional entities, surpassing the limitations of previous methods. The versatility of the radical pathway is further demonstrated through straightforward three-component reactions involving alkenes and [1.1.1]propellane. Detailed experimental and computational studies have elucidated the origins of regioselectivity, providing profound insights into the mechanistic aspects.

The incorporation of fluoroalkyl groups into molecular frameworks represents a pivotal advancement in synthetic organic chemistry, profoundly impacting drug design¹⁻⁵ and agrochemical applications^{6,7}. These groups, characterized by their high bond dissociation energies and the marked polarity of the C–F bond, enhance metabolic stability and modulate cellular membrane permeability⁸⁻¹⁰. For instance, a difluoroethyl group effectively replicates the steric and electronic properties of a methoxy group, significantly improving the potency and metabolic durability of compounds (Fig. 1a)¹¹. The strategic incorporation of fluoroalkyl groups as versatile bioisosteres for various functional groups refines the physical and chemical properties of molecules, expanding their utility in the development of novel therapeutics and agrochemicals, thereby facilitating the generation of more robust and effective chemical entities^{12,13}.

Pyridines, prominently featured in pharmaceuticals, are critical in drug development^{14,15}, with pyridyl C–H fluoroalkylation playing a key role in bioisosteric designs¹⁶⁻¹⁷. Traditionally, the formation of pyridyl C–CF₂X bonds predominantly relied on transition metal-catalyzed cross-coupling¹⁸⁻²² and C–H functionalization reactions²³. The resurgence of Minisci-type radical processes and advancements in photocatalysis have paved the way for alternative methodologies that modify these reactions²⁴⁻²⁷. These radical C–H functionalization reactions, despite a consistent mechanism, struggle with controlling regioselectivity and reactivity, heavily influenced by the substituents on the pyridine and the reaction conditions (Fig. 1b, left)²⁸. Recently, McNally and colleagues reported a breakthrough in C4-selective fluoroalkylation using fluoroalkylphosphonium salts through a two-electron pathway, representing the first instance of regiocontrolled fluoroalkylation of pyridines using fluoroalkylphosphines as reagents (Fig. 1b, right)^{29,30}. While innovative, this method is limited by the multi-step synthesis of fluoroalkylphosphines and the difficulty in accessing CF₂-alkyl groups with diverse functional groups.

To date, the relatively limited range of readily available fluoroalkyl radical sources, particularly those capable of efficiently generating CF₂-alkyl radicals with diverse functional groups, has posed a challenge in the development of photoinduced methods for the direct incorporation of these valuable moieties into pyridines. These limitations highlight the need for new, more versatile reaction methodologies that can efficiently incorporate a broader range of fluoroalkyl groups into pyridines. To overcome these limitations, we propose utilizing readily available and bench stable sulfinates as fluoroalkyl sources, combined with *N*-pyridinium salts for C4-selective incorporation of diverse fluoroalkyl groups into pyridines (Fig. 1C).³¹ Employing electron donor-acceptor (EDA) complexes, our strategy achieves high selectivity and broad applicability under mild conditions, eliminating the need for an external photocatalyst^{32,33}. Our approach not only enables the effective installation of CF₂H groups into complex pyridine-containing substrates but also allows for the incorporation of CF₂-alkyl groups with diverse functional groups, significantly expanding the chemical space available for cutting-edge pharmaceutical and agrochemical research. Furthermore, by leveraging the photoinduced radical mechanism, our method enables efficient three-component difunctionalization of useful linker motifs, such as alkenes³⁴ and [1.1.1]propellane^{35,36}, thereby providing a valuable tool for the synthesis of diverse fluoroalkylated azines.

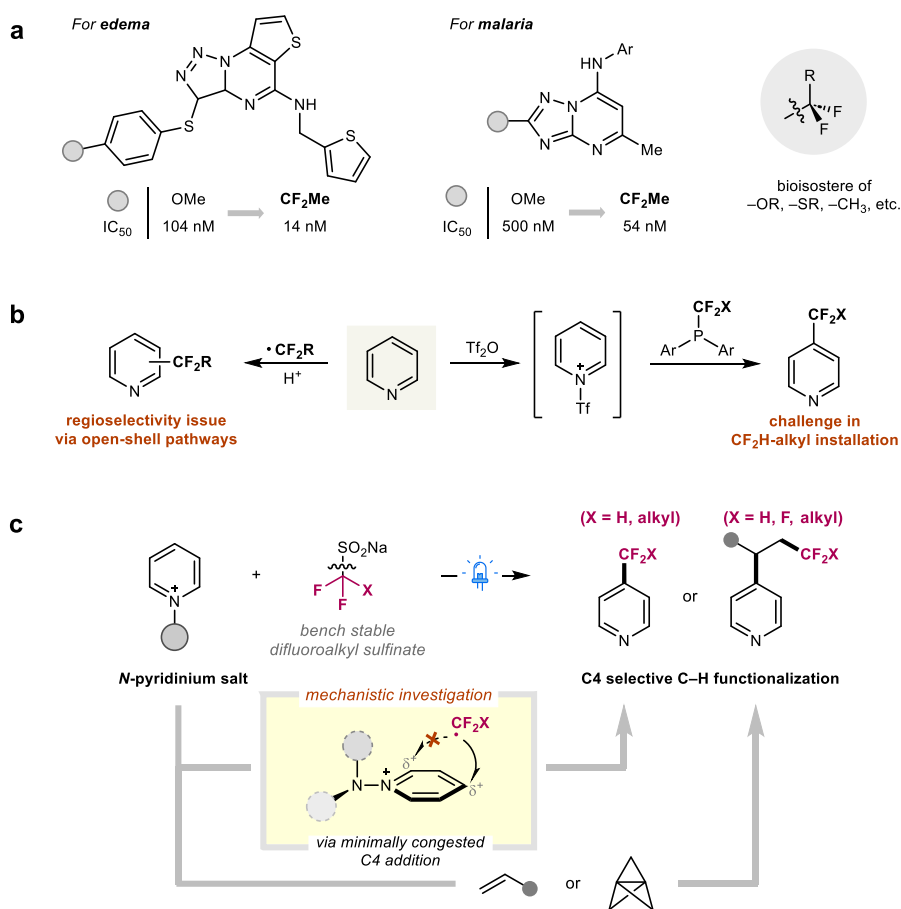


Fig. 1 | Design plan for photoinduced C4-selective fluoroalkylation of pyridines. **a**, Representative examples of fluoroalkyl groups as a bioisosteres for the methoxy group. **b**, Synthetic routes to fluoroalkylated pyridines via Minisci-type reactions (left) and phosphine reagents for C4-selective fluoroalkylation of pyridines (right). **c**, Our strategy for radical-mediated C4-selective fluoroalkylation and three-component reactions of pyridines (CF₃, CF₂H, and CF₂-alkyl groups).

RESULTS & DISCUSSION

Reaction optimization. To implement the design plan, we evaluated the viability of our approach employing *N*-aminopyridinium salt **PG1** and sodium sulfinate **2a** as model substrates under blue LED irradiation (Table 1). In this study, the difluoromethyl radical was selected as the optimal candidate for investigating regioselectivity due to its minimal steric hindrance³⁷. The fluoroalkyl sulfinate functions as a radical precursor through single electron oxidation, leading to the release of sulfur dioxide (SO₂) and the generation of CF₂H radicals. We propose that upon observing an interaction between the *N*-aminopyridinium salt and the sulfinate in their ground states, excitation of the resultant EDA complex will facilitate the generation of CF₂H radicals³⁸. Following the optimization of key parameters, the desired product **3a** was synthesized in an impressive 83% yield, without the need for external photocatalysts or additives (entry 1). Among the solvents tested, dimethyl sulfoxide (DMSO) proved to be the most effective, while alternative solvents resulted in lower yields (entries 2 and 3). The use of different CF₂H radical precursors, such as difluoroacetate³⁹ and Baran's reagent (zinc

difluoromethanesulfinate, DFMS)⁴⁰⁻⁴¹, led to decreased or no reactivity (entries 4 and 5). Our exploration extended to various pyridinium salts featuring diverse *N*-substituents, with the aim of assessing the impact of the *N*-substituent on regioselectivity. Replacing salt **PG1** with **PG2** markedly reduced regioselectivity, underscoring the critical role of a sterically hindered sulfonyl group in achieving C4-selectivity (entry 6). Furthermore, the incorporation of an alkyl substituent in the sulfonamide group proved vital for site-selective product formation (entry 7). To assess the impact of the tolyl group on selectivity, we examined different substitutions on the sulfonyl group (Supplementary Table 1). Notably, the selectivity remained consistent regardless of the presence of a phenyl ring, indicating its minimal influence on selectivity (entry 8). Intriguingly, substituting the amidyl group with a methoxy group as the *N*-substituent in the pyridine reversed the selectivity, resulting in the production of **3a** and **3a'** in a ratio of 1:1.1 (entry 9). Control experiments confirmed that light is essential for the reaction to proceed (entry 10), while conducting the reaction in an air atmosphere reduced the efficiency (entry 11).

Entry	Variations	% Yield (3a+3a')	Selectivity (3a:3a')
1	None	83	> 99:1
2	DCM instead of DMSO	49	> 99:1
3	MeCN instead of DMSO	44	> 99:1
4	NaCO ₂ CF ₂ H instead of 2a	n.d.	-
5	Zn(SO ₂ CF ₂ H) ₂ instead of 2a	38	> 99:1
6	PG2 instead of PG1	38	12:1
7 ^a	PG3 instead of PG1	3	2:1
8	PG4 instead of PG1	36	> 99:1
9	PG5 instead of PG1	49	1:1.1
10	without blue LEDs	n.d.	-
11	Air instead of Ar	60	> 99:1

Table 1 | Reaction optimization of C4-selective difluoromethylation. Reaction conditions: *N*-pyridinium salt (0.075 mmol), sodium sulfinate **2a** (0.05 mmol) in DMSO (1.0 mL) under irradiation using a Penn PhD photoreactor M2 ($\lambda_{\text{max}} = 450$ nm) under an argon atmosphere at room temperature for 16 h. The yield and selectivity were determined by ¹⁹F NMR spectroscopy with PhCF₃ as an internal standard. ^a9-Mesityl-10-methylacridinium perchlorate was used as a photocatalyst.

To assess the site-selectivity afforded by our developed methodology, we conducted a comparative analysis with established radical-mediated reactions (Fig. 2). Three distinct azine substrates, each featuring both reactive *para* and *ortho* C–H bonds—2-phenylpyridine, quinoline, and vismodegib—were chosen for this investigation. Under light irradiation and using difluoromethylsulfinate alongside *N*-aminopyridinium salts, the difluoromethylated products were obtained with

yields of 83%, 96%, and 80%, respectively, demonstrating outstanding *para/ortho* selectivity ranging from 80:1 to over 99:1. These results were then benchmarked against data from four conventional radical-mediated C–H difluoromethylation techniques (denoted as B through E). We explored azine derivatives including *N*-methoxy- and *N*-oxide pyridinium salts (methods B and C⁴²) as well as Minisci-type acidified azines (methods D⁴⁰ and E⁴³). Notably, compared to the use of *N*-aminopyridinium salts, which showed superior *para*-selectivity, these derivatives exhibited decreased regioselectivity and reactivity. The findings presented in Fig. 2 emphasize the marked C4 site-selectivity achieved by our approach, paving the way for new strategies in selective C–H difluoromethylation within intricate molecular architectures.

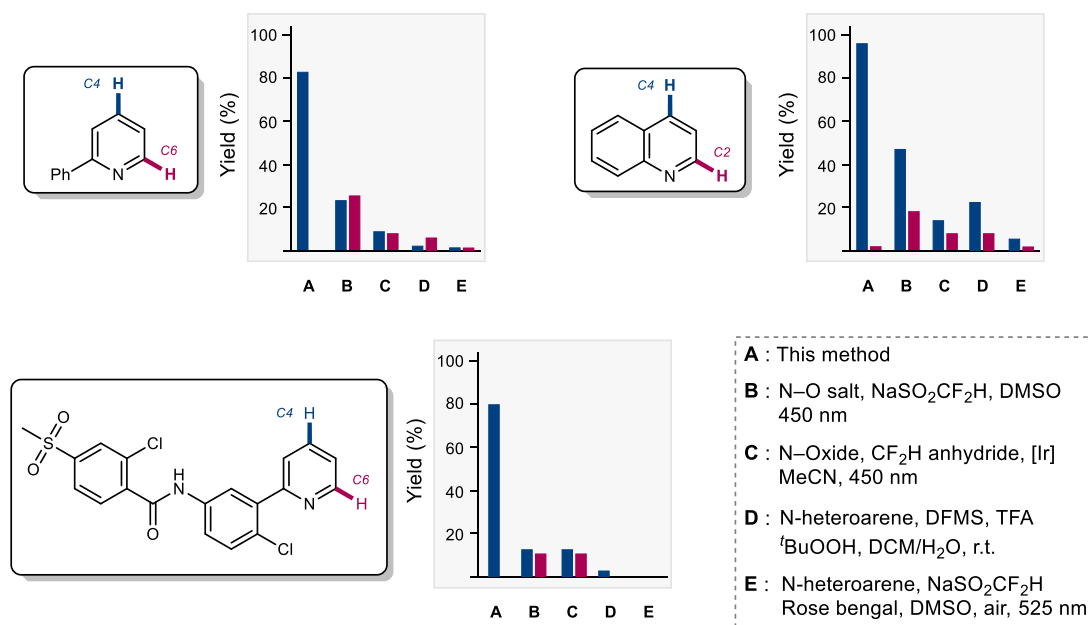


Fig. 2 | Comparison of difluoromethylation site-selectivity using various radical-mediated methods.

Mechanistic Investigation. To elucidate the regioselectivity observed in C4 difluoromethylation, we employed quantum chemical methods at the M062X/def2-QZVPP//B3LYP-D3/def2-TZVP level of theory. Regioselectivity in nucleophilic radical additions is often assessed through differences in atomic charges or LUMO coefficients. Our findings indicate that while the C6 position exhibits a higher positive charge compared to the C4 position, the LUMO coefficient for compound **PG1** is notably higher at C4 than at C6, as shown in Fig. 3a. This disparity in electronic properties underscores the multifaceted nature of factors influencing regioselectivity in this reaction system. Before initiating the calculations, we selected the difluoromethyl radical as a model substrate due to its nucleophilic nature among common alkyl radicals, its minimal steric hindrance, and reduced interactions. By studying the difluoromethyl radical, we aim to provide insights into the factors governing the regioselectivity not only for difluoromethylation but also for the addition of unactivated alkyl radicals to *N*-aminopyridinium salts. To further elucidate the underlying mechanism governing this selectivity, we conducted kinetic isotope effect (KIE) experiments to determine the rate-determining step (Fig. 3b). Comparative

experiments involving **PG1** and C4-deuterated **PG1-D** under standard conditions, with initial rate assessments conducted after 20 minutes, yielded an inverse secondary KIE of 0.954. This finding indicates that the C–H bond cleavage of C4 position is not rate-determining step of this transformation, deviating from the typical pathways observed in Minisci-type radical reactions⁴⁴. The inverse secondary KIE suggests that the addition of the difluoromethyl radical to the *N*-aminopyridinium salt is likely to rate-limiting in this transformation.

Additionally, to corroborate our experimental findings, we conducted Density Functional Theory (DFT) calculations to simulate the radical addition process (Fig. 3c). The computed transition state energies demonstrated that the addition at C4 is energetically more favorable than at C6 by approximately 1.6 kcal/mol. Interestingly, the radical addition to both C4 and C6 positions was found to be more favorable when the sulfonyl protecting group was oriented away from the incoming radical (Supplementary Table 2). This observation underscores the significant influence of the sulfonyl group on regioselectivity, as demonstrated in the optimization experiments. The geometries of these transition states are depicted in Fig. 3d. Non-covalent interaction plots reveal that the less favored C6 transition state experiences significant steric 1,3-strain, attributed to the close proximity of the difluoromethyl radical to the methyl group on the *N*-substituent. A distortion-interaction analysis provided further insights into the factors contributing to the observed regioselectivity. While the distortion energies for the C4 transition state were lower by 1.3 kcal/mol, the interaction energies were only marginally different by 0.2 kcal/mol (Fig. 3e). The increased torsional strain observed in the C6 transition state, aimed at mitigating steric interactions, highlights the crucial role of steric hindrance in dictating the regioselectivity observed in the formation of compound **3a**. These computational studies, in conjunction with our experimental findings, provide a comprehensive understanding of the factors governing the C4 selectivity in the alkylation of *N*-aminopyridinium salts⁴⁵⁻⁴⁷. The interplay between electronic properties, steric effects, and the influence of the sulfonyl group on the transition state geometries collectively contribute to the observed regioselectivity.

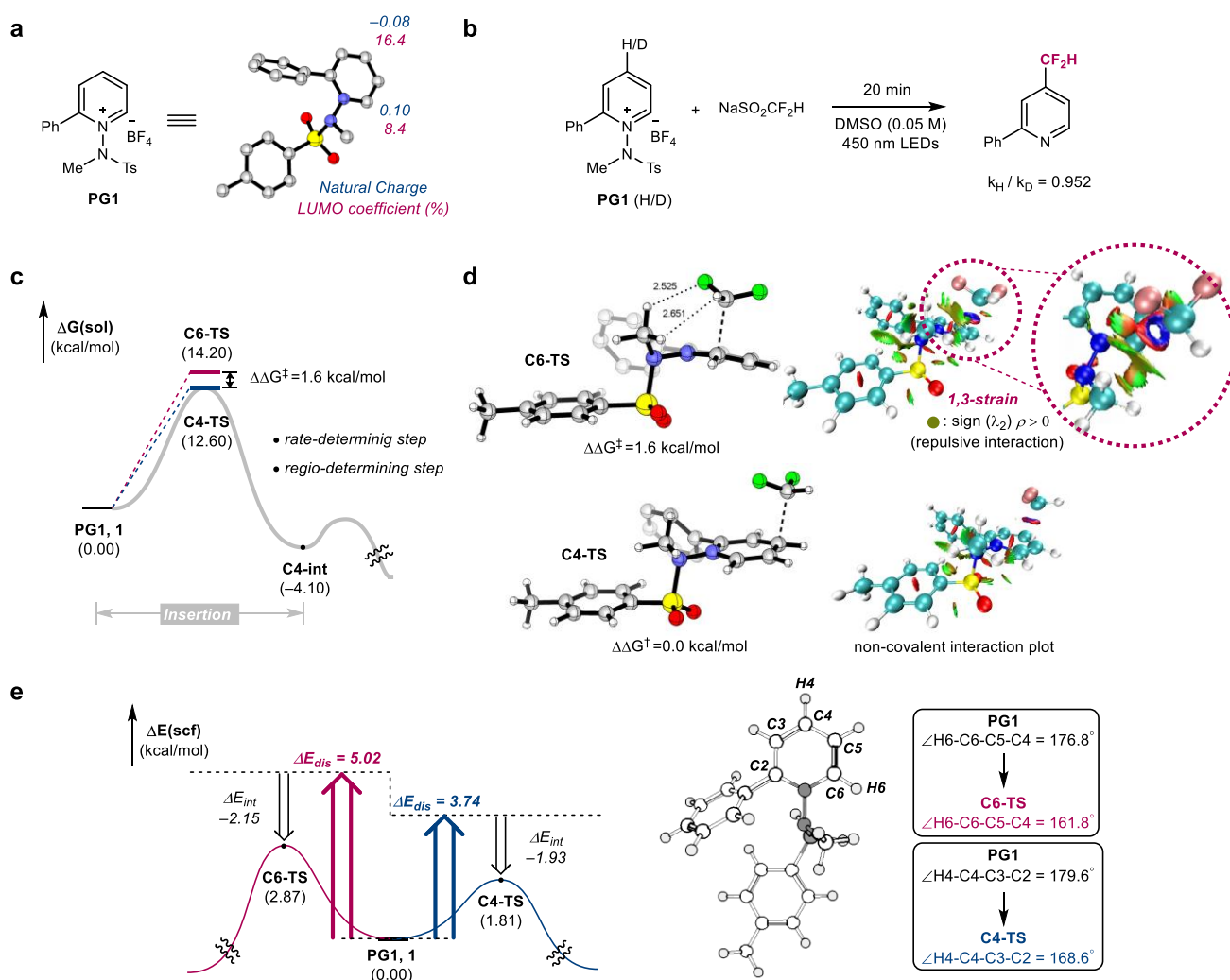


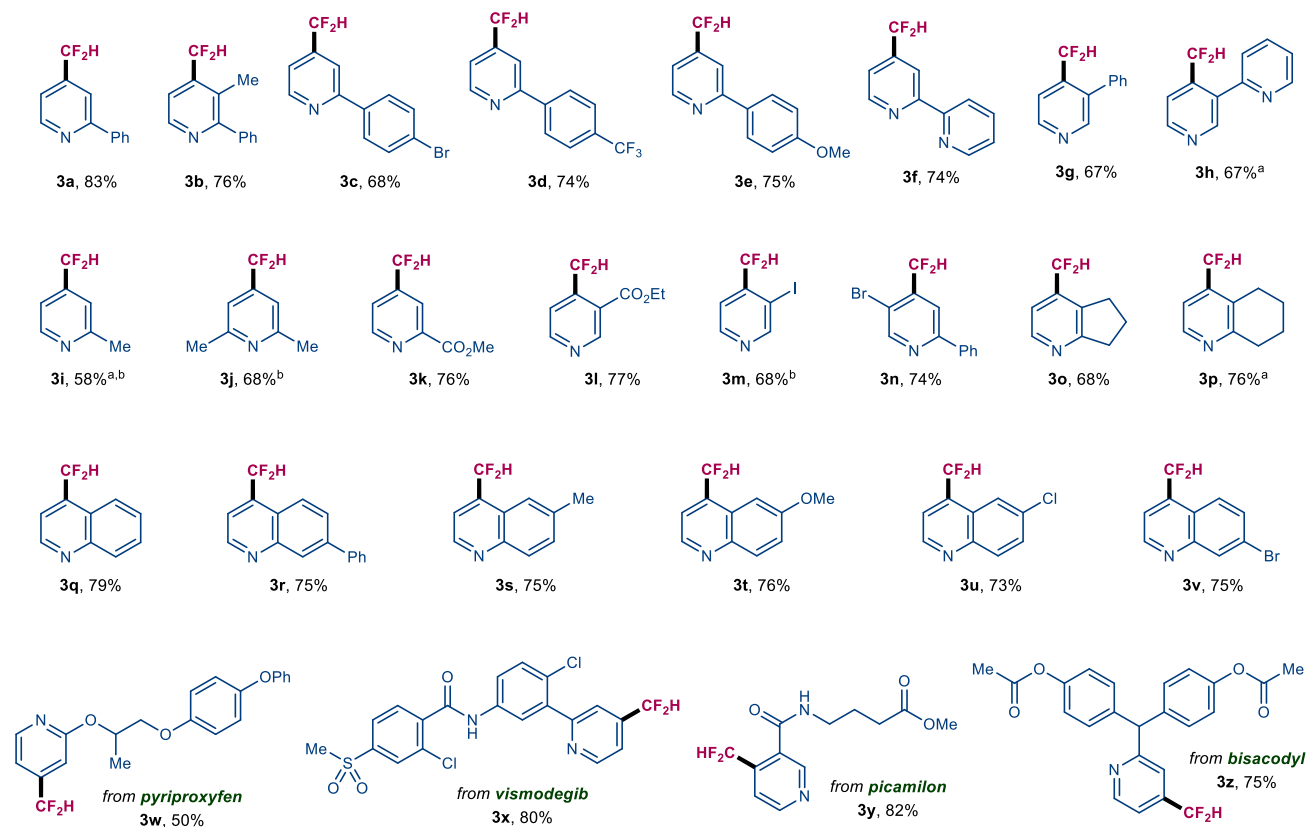
Fig. 3 | Experimental and computational investigation of regioselectivity. **a**, Electronic properties of **PG1**, showing the LUMO coefficients and atomic charges at the C4 and C6 positions. **b**, Kinetic isotope effect (KIE) experiment comparing the reaction rates of **PG1** and C4-deuterated **PG1-D**, revealing an inverse secondary KIE. **c**, Computed energy profile of the radical addition at the C4 and C6 positions, demonstrating the energetic preference for C4 addition. **d**, Non-covalent interaction plot of transition states for radical addition at C4 and C6. **e**, Distortion-interaction analysis of transition states for radical addition, quantifying the contributions of distortion and interaction energies to the overall energy difference between the C4 and C6 transition states.

Substrate scope. Building on prior experimental and computational insights, we expanded the investigation to encompass various pyridines and fluoroalkanes. To our delight, various 2-phenylpyridine derivatives showed excellent C4-selectivity (**3a** and **3b**). This effect was systematically examined across a variety of *N*-pyridinium substrates that featured electronically diverse substitutions at the C2-phenyl ring, including *p*-bromo (**3c**), *p*-trifluoromethyl (**3d**), and *p*-methoxy (**3e**) groups. These substrates efficiently underwent difluoromethylation, showcasing the robustness of the reaction under these conditions. Despite the potential influence of the bipyridine framework on reactivity and selectivity, the reaction successfully produced the desired product **3f**. Expanding the scope of our investigation, we explored C3-substituted

substrates and successfully obtained the desired products (**3g** and **3h**). Moreover, pyridinium salts adorned with either mono- (**3i**) or dialkyl (**3j**) groups were also found to be compatible with the developed methodology, thus broadening the substrate applicability. Notably, substrates equipped with electron-withdrawing groups such as esters (**3k**, **3l**) were effectively engaged in this transformation. This observation underscores the pronounced nucleophilicity of difluoroalkyl radicals, which can engage even electron-deficient pyridine units, thereby facilitating a broad range of transformations. The robustness of functional groups commonly involved in cross-coupling reactions—specifically iodo (**3m**) and bromo (**3n**) groups—was maintained, reflecting the mild nature of the reaction conditions. This protocol was not only successful with cyclic substrates (**3o** and **3p**) but was also aptly extended to quinoline cores (**3q**), which proceeded with the reaction smoothly and effectively. Significantly, quinolines substituted with various groups such as phenyl (**3r**), methyl (**3s**), methoxy (**3t**), and halides (**3u** and **3v**) reacted smoothly, demonstrating the method's versatility and efficiency. The late-stage functionalization of complex drug molecules further highlighted the broad synthetic utility of our protocol (**3w–3z**), demonstrating its potential for streamlined synthesis and modifications in medicinal chemistry applications. In all cases, exclusive C4 selectivity was obtained, underscoring the precision of the reaction under the standard conditions. We then extended our investigation to assess the robustness of this methodology with respect to the incorporation of CF₂-alkyl groups. Notably, this approach enables the synthesis of products that were previously inaccessible using conventional methods. An examination involving a variety of commercially available difluoroalkyl sulfinates, featuring alkyl (**3aa–3ac**) or aryl (**3ad**) substituents, demonstrated exceptional site-selectivity not only towards simple pyridine units but also within intricate molecular frameworks. The successful incorporation of fluoroalkanes into diverse drug molecules (**3ae–3ah**) exemplifies remarkable functional group tolerance, representing a considerable promise for advancing drug discovery and development, potentially leading to the development of more efficacious pharmaceuticals. The broad substrate scope, encompassing a wide array of fluoroalkanes, highlights the generality and robustness of our methodology. To further demonstrate the potential of this transformation for late-stage functionalization, we applied this methodology to the derivatization of biologically active molecules, as presented in Table 2.



N-heteroarenes



CF₂-alkyl groups

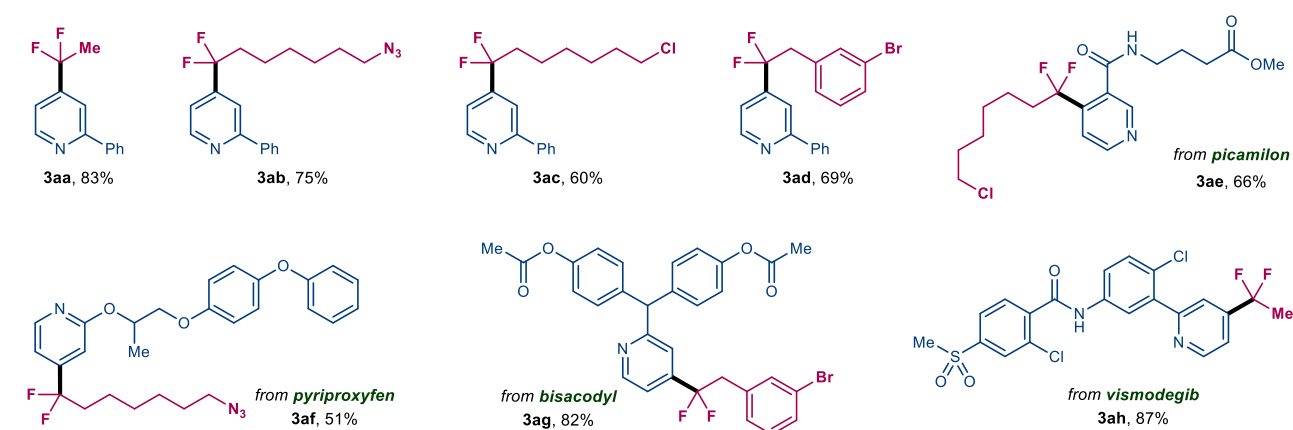
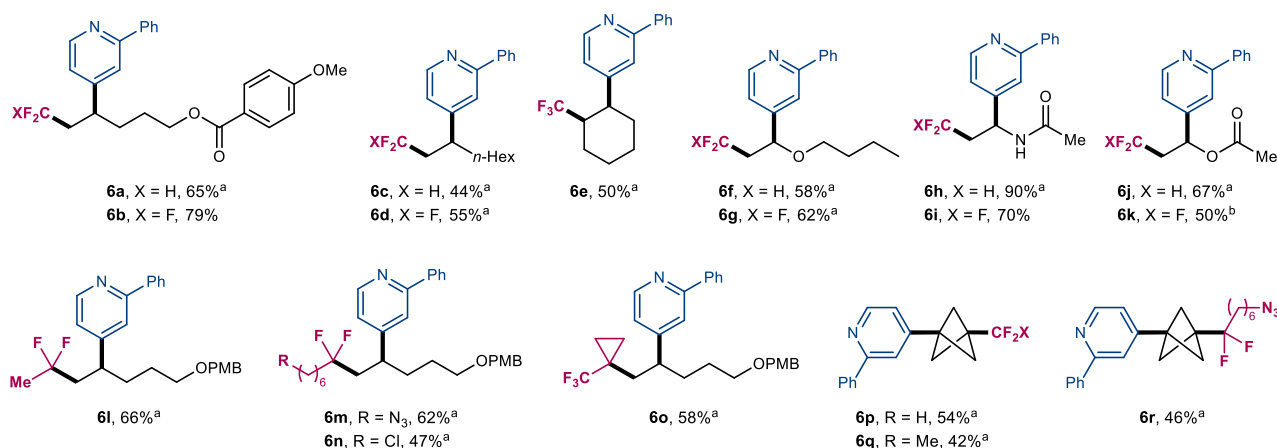
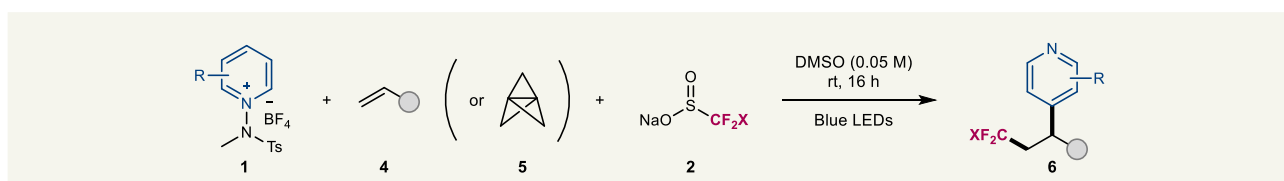


Table 2 | Substrate scope of fluoroalkylation. Reaction conditions: *N*-aminopyridinium salt **1** (0.075 mmol), and sodium sulfinate **2** (0.05 mmol) in DMSO (1.0 mL) under irradiation using a Penn PhD photoreactor M2 ($\lambda_{\text{max}} = 450$ nm) under an argon atmosphere at room temperature for 16 h. ^aPG6 was used instead of PG1. ^bThe compound was not isolated due to its volatility; yields were determined by ¹H NMR spectroscopy with caffeine as an internal standard. The *para/ortho* selectivity is >20:1 for all cases.

To assess the versatility of our methodology, we undertook an examination of radical cascade reactions, focusing on the straightforward three-component difunctionalization involving alkenes and [1.1.1]propellane (Table 3). In these studies, difluoromethyl, trifluoromethyl, and difluoroalkyl radicals were tested to afford various potential bioisosteres. In certain cases, an appropriately selected base (NaHCO_3 or KHCO_3) was added during these reactions to facilitate deprotonation and promote homolytic N–N bond cleavage. This method proved to be broadly applicable across a diverse spectrum of alkenes, demonstrating excellent tolerance to a wide range of functional groups. For instance, unactivated alkenes featuring carbonyl functionalities showed good performance under standard reaction conditions (**6a** and **6b**). Similarly, simple alkenes, such as octene (**6c** and **6d**) and cyclohexene (**6e**), also proved suitable. Furthermore, a diverse array of alkenes, characterized by the presence of ether (**6f** and **6g**), amide (**6h** and **6i**), and ester (**6j** and **6k**) functional groups, successfully participated in these reactions. Our further exploration into the generality of this approach with respect to fluoroalkanes revealed that a variety of commercially available difluoroalkyl sulfinates were compatible with the process (**6l–6n**). Notably, our protocol facilitated the incorporation of strained trifluoromethyl-cyclopropyl groups, which are pharmaceutically relevant (**6o**)⁴⁸. Moreover, using [1.1.1]propellane as a linker, our methodology extended to difluoromethylpyridylation, effectively synthesizing 1,3-functionalized bicyclo[1.1.1]pentane (BCP) building blocks (**6p–6r**). These BCP derivatives have garnered significant interest in medicinal chemistry due to their unique structural and physicochemical properties, which can enhance drug-like characteristics such as metabolic stability and bioavailability^{49,50}. Lastly, the practicality of conducting multicomponent cascade reactions was demonstrated by the successful implementation of late-stage C–H fluoroalkylation. The site-selective fluoroalkylpyridylation could be extended to vismodegib (**6s** and **6t**), picamilon (**6u** and **6v**), bisacodyl (**6w** and **6x**), and pyriproxyfen (**6y**) derivatives, highlighting the functional group compatibility.



late-stage functionalization

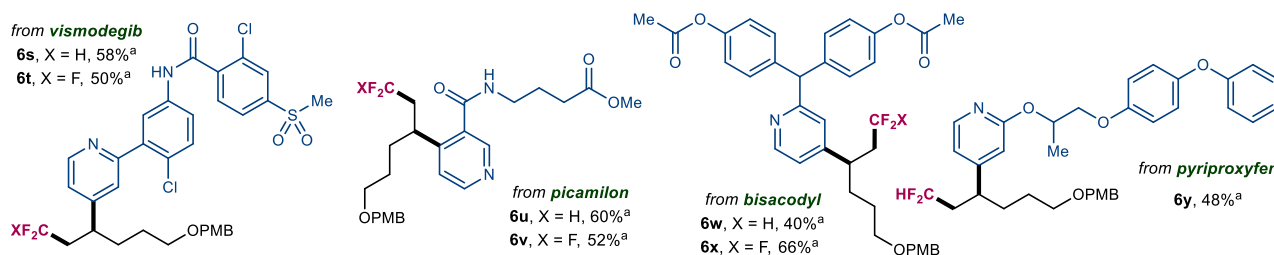


Table 3 | Substrate scope of the three-component fluoroalkyl pyridylation. Reaction conditions: *N*-aminopyridinium salt **1** (0.075 mmol), sodium sulfinatate **2** (0.05 mmol), and alkene **4** or [1.1.1]propellane **5** (0.05 mmol) in DMSO (1.0 mL) under irradiation using a Penn PhD photoreactor M2 ($\lambda_{\text{max}} = 450 \text{ nm}$) under an argon atmosphere at room temperature for 16 h. PMB = *para*-methoxybenzoyl. ^aKHCO₃ (1.2 eq) or ^bNaHCO₃ (1.2 eq) were used as an additive. The *para/ortho* selectivity is >20:1 for all cases.

CONCLUSIONS

In conclusion, we have developed a highly efficient method for the C4-selective fluoroalkylation of pyridines and quinolines using readily available sulfinates combined with *N*-amidopyridinium salts. Our method not only facilitates the installation of CF₂H groups but also enables the incorporation of functionally diverse CF₂-alkyl groups, which is of paramount importance in the pharmaceutical and agrochemical industries. By employing EDA complexes, our method achieves broad applicability under mild, photocatalyst-free conditions, effectively overcoming previous limitations associated with the preparation of fluoroalkyl sources. Furthermore, the integration of a photoinduced radical mechanism enables the versatile difunctionalization of useful linker motifs, such as alkenes and [1.1.1]propellane, for the synthesis of various fluoroalkylated azines. Our comprehensive experimental and computational investigations provide valuable

insights into the factors governing C4-selectivity, laying the foundation for a more rational approach to site-selective pyridine functionalization strategies. This work enables the synthesis of a wide array of potential fluoroalkyl-containing azine bioisosteres, which can significantly enhance the pharmacological properties of drug candidates, ultimately leading to the development of novel therapeutics and functional materials with improved properties and performance.

METHODS

Fluoroalkylation: In an argon-filled glove box, *N*-aminopyridinium salt **1** (1.5 equiv, 0.075 mmol), sodium sulfinate **2** (1 equiv, 0.05 mmol), and anhydrous DMSO (0.05 M, 1.0 mL) were added to a 12 mL test tube equipped with a magnetic stir bar. The sealed test tube was placed in a Penn PhD Photoreactor M2 and stirred at room temperature for 16 h. The resulting mixture was diluted with EtOAc and washed with H₂O. The aqueous layer was extracted with EtOAc three times. The combined organic layers were dried over sodium sulfate, filtered, and concentrated under reduced pressure. The residue was purified by flash column chromatography on silica gel to afford the final product.

Three-component reaction: In an argon-filled glove box, *N*-aminopyridinium salt **1** (1.5 equiv, 0.075 mmol), sodium sulfinate **2** (1 equiv, 0.05 mmol), and anhydrous DMSO (0.05 M, 1.0 mL) were added to a 12 mL test tube equipped with a magnetic stir bar. The sealed test tube was placed in a Penn PhD Photoreactor M2 and stirred at room temperature for 16 h. The resulting mixture was diluted with EtOAc and washed with H₂O. The aqueous layer was extracted with EtOAc three times. The combined organic layers were dried over sodium sulfate, filtered, and concentrated under reduced pressure. The residue was purified by flash column chromatography on silica gel to afford the final product.

DATA AVIALABILITY

Experimental procedure and characterization data of new compounds are available within Supplementary Information. Computational details, optimized Cartesian coordinates of all structures, vibrational frequencies, and energy components. This material is available free of charge via the Internet.

REFERENCES

1. Gillis, E. P., Eastman, K. J., Hill, M. D., Donnelly, D. J. & Meanwell, N. A. Applications of Fluorine in Medicinal Chemistry. *J. Med. Chem.* **58**, 8315–8359 (2015).

2. Zhou, Y. *et al.* Next Generation of Fluorine-Containing Pharmaceuticals, Compounds Currently in Phase II-III Clinical Trials of Major Pharmaceutical Companies: New Structural Trends and Therapeutic Areas. *Chem. Rev.* **116**, 422–518 (2016).
3. Müller, K., Faeh, C. & Diederich, F. Fluorine in pharmaceuticals: looking beyond intuition. *Science* **317**, 1881–1886 (2007).
4. Hagmann, W. K. The many roles for fluorine in medicinal chemistry. *J. Med. Chem.* **51**, 4359–4369 (2008).
5. Wang, J. *et al.* Fluorine in pharmaceutical industry: fluorine-containing drugs introduced to the market in the last decade (2001–2011). *Chem. Rev.* **114**, 2432–2506 (2014).
6. Jeschke, P. The unique role of fluorine in the design of active ingredients for modern crop protection. *Chembiochem* **5**, 571–589 (2004).
7. Burriss, A. *et al.* The importance of trifluoromethyl pyridines in crop protection. *Pest Manag. Sci.* **74**, 1228–1238 (2018).
8. Zafrani, Y. *et al.* CF₂H, a Functional Group-Dependent Hydrogen-Bond Donor: Is It a More or Less Lipophilic Bioisostere of OH, SH, and CH₃? *J. Med. Chem.* **62**, 5628–5637 (2019).
9. Levi, N., Amir, D., Gershonov, E. & Zafrani, Y. Recent Progress on the Synthesis of CF₂H-Containing Derivatives. *Synthesis* **51**, 4549–4567 (2019).
10. O'Hagan, D. Understanding organofluorine chemistry. An introduction to the C-F bond. *Chem. Soc. Rev.* **37**, 308–319 (2008).
11. Zhou, Q. *et al.* Direct synthesis of fluorinated heteroarylether bioisosteres. *Angew. Chem. Int. Ed.* **52**, 3949–3952 (2013).
12. Wu, S., Wu, X., Wang, D., Zhu, C. Regioselective vinylation of remote unactivated C(sp³)-H bonds: access to complex fluoroalkylated alkenes. *Angew. Chem. Int. Ed.* **58**, 1499–1503 (2019).
13. Wang, Z.-X. *et al.* Regioselective, catalytic 1,1-difluorination of enynes. *Nat. Chem.* **15**, 1515–1522 (2023).
14. Vitaku, E., Smith, D. T. & Njardarson, J. T. Analysis of the structural diversity, substitution patterns, and frequency of nitrogen heterocycles among U.S. FDA approved pharmaceuticals. *J. Med. Chem.* **57**, 10257–10274 (2014).

15. A. F. Pozharskii, A. T. Soldatenkov, A. R. Katritzky, *Heterocycles in Life and Society: An Introduction to Heterocyclic Chemistry, Biochemistry, and Applications*, 2nd ed., Wiley, Hoboken, 2011, p. 139–143.
16. Jeppsson, F. *et al.* Discovery of AZD3839, a potent and selective BACE1 inhibitor clinical candidate for the treatment of Alzheimer disease. *J. Biol. Chem.* **287**, 41245–41257 (2012).
17. Luo, G. *et al.* Discovery of (S)-1-((2',6-Bis(difluoromethyl)-[2,4'-bipyridin]-5-yl)oxy)-2,4-dimethylpentan-2-amine (BMS-986176/LX-9211): A Highly Selective, CNS Penetrable, and Orally Active Adaptor Protein-2 Associated Kinase 1 Inhibitor in Clinical Trials for the Treatment of Neuropathic Pain. *J. Med. Chem.* **65**, 4457–4480 (2022).
18. Bacauanu, V. *et al.* Metallaphotoredox Difluoromethylation of Aryl Bromides. *Angew. Chem. Int. Ed.* **57**, 12543–12548 (2018).
19. Lu, C., Gu, Y., Wu, J., Gu, Y. & Shen, Q. Palladium-catalyzed difluoromethylation of heteroaryl chlorides, bromides and iodides. *Chem. Sci.* **8**, 4848–4852 (2017).
20. Xu, L. & Vicic, D. A. Direct Difluoromethylation of Aryl Halides via Base Metal Catalysis at Room Temperature. *J. Am. Chem. Soc.* **138**, 2536–2539 (2016).
21. Zhang, X.-Y. *et al.* Reductive Catalytic Difluorocarbene Transfer via Palladium Catalysis. *Angew. Chem. Int. Ed.* **62**, e202306501 (2023).
22. Zhao, H., Leng, X. B., Zhang, W. & Shen, Q. $[\text{Ph}_4\text{P}]^+[\text{Cu}(\text{CF}_2\text{H})_2]^-$: A Powerful Difluoromethylating Reagent Inspired by Mechanistic Investigation. *Angew. Chem. Int. Ed.* **61**, e202210151 (2022).
23. Cao, P., Duan, J.-X. & Chen, Q.-Y. Difluoroiodomethane: practical synthesis and reaction with alkenes. *J. Chem. Soc. Chem. Commun.* 737–738 (1994).
24. Nagib, D. A. & MacMillan, D. W. C. Trifluoromethylation of arenes and heteroarenes by means of photoredox catalysis. *Nature* **480**, 224–228 (2011).
25. Yuan, J. *et al.* Visible-Light-Induced Cascade Cyclization of 1-Acryloyl-2-cyanoindole: Access of Difluoroalkylated Pyrrolo[1,2-a]indoleiones. *J. Org. Chem.* **88**, 16598–16608 (2023).
26. Xu, Y. *et al.* Photoredox-Catalyzed Three-Component Difluoroalkylation of Quinoxalin-2(1H)-ones with Unactivated Vinylarenes and $[\text{Ph}_3\text{PCF}_2\text{H}]^+\text{Br}^-$. *Asian Journal of Organic Chemistry* **12**, e202300405 (2023).
27. Beatty, J. W., Douglas, J. J., Cole, K. P. & Stephenson, C. R. J. A scalable and operationally simple radical trifluoromethylation. *Nat. Commun.* **6**, 7919 (2015).

28. O'Hara, F., Blackmond, D. G. & Baran, P. S. Radical-Based Regioselective C–H Functionalization of Electron-Deficient Heteroarenes: Scope, Tunability, and Predictability. *J. Am. Chem. Soc.* **135**, 12122–12134 (2013).
29. Hilton, M. C., Dolewski, R. D. & McNally, A. Selective Functionalization of Pyridines via Heterocyclic Phosphonium Salts. *J. Am. Chem. Soc.* **138**, 13806–13809 (2016).
30. Zhang, X. *et al.* Phosphorus-mediated sp²-sp³ couplings for C-H fluoroalkylation of azines. *Nature* **594**, 217–222 (2021).
31. While preparing our manuscript for submission, we encountered a recently published article reporting the introduction of CF₂H radical into pyridine utilizing 2,2-difluoro-2-iodo-1-phenylethan-1-one or bis(difluoroacetyl) peroxide as the radical source. See: Xu, P., Wang, Z., Guo, S.-M. & Studer, A. Introduction of the difluoromethyl group at the meta- or para-position of pyridines through regioselectivity switch. *Nat. Commun.* **15**, 4121 (2024).
32. James, M. J. *et al.* Visible-Light-Mediated Charge Transfer Enables C–C Bond Formation with Traceless Acceptor Groups. *Chemistry* **25**, 8240–8244 (2019).
33. Quint, V. *et al.* Visible-light-mediated α -phosphorylation of N-aryl tertiary amines through the formation of electron-donor–acceptor complexes: synthetic and mechanistic studies. *Org. Chem. Front.* **6**, 41–44 (2018).
34. Lee, K., Lee, S., Kim, N., Kim, S. & Hong, S. Visible-Light-Enabled Trifluoromethylative Pyridylation of Alkenes from Pyridines and Triflic Anhydride. *Angew. Chem. Int. Ed.* **59**, 13379–13384 (2020).
35. Shin, S., Lee, S., Choi, W., Kim, N. & Hong, S. Visible-Light-Induced 1,3-Aminopyridylation of [1.1.1]Propellane with *N*-Aminopyridinium Salts. *Angew. Chem. Int. Ed.* **60**, 7873–7879 (2021).
36. Wu, Z., Xu, Y., Liu, J., Wu, X. & Zhu, C. A practical access to fluoroalkylthio(seleno)-functionalized bicyclo[1.1.1]pentanes. *Sci. China Chem.* **8**, 1025–1029 (2020).
37. Parsaee, F. *et al.* Radical philicity and its role in selective organic transformations. *Nat Rev Chem* **5**, 486–499 (2021).
38. Kim, M., You, E., Park, S. & Hong, S. Divergent reactivity of sulfinates with pyridinium salts based on one- versus two-electron pathways. *Chem. Sci.* **12**, 6629–6637 (2021).
39. Tung, T. T., Christensen, S. B. & Nielsen, J. Difluoroacetic Acid as a New Reagent for Direct C-H Difluoromethylation of Heteroaromatic Compounds. *Chem. Eur. J.* **23**, 18125–18128 (2017).
40. Fujiwara, Y. *et al.* A new reagent for direct difluoromethylation. *J. Am. Chem. Soc.* **134**, 1494–1497 (2012).

41. Fujiwara, Y. *et al.* Practical and innate carbon-hydrogen functionalization of heterocycles. *Nature* **492**, 95–99 (2012).
42. Sun, A. C., McClain, E. J., Beatty, J. W. & Stephenson, C. R. J. Visible Light-Mediated Decarboxylative Alkylation of Pharmaceutically Relevant Heterocycles. *Org. Lett.* **20**, 3487–3490 (2018).
43. Zhang, W. *et al.* Direct C-H difluoromethylation of heterocycles via organic photoredox catalysis. *Nat. Commun.* **11**, 638 (2020).
44. Jiang, Y.-X. *et al.* Visible-light-driven synthesis of N-heteroaromatic carboxylic acids by thiolate-catalysed carboxylation of C(sp²)-H bonds using CO₂. *Nat. Synth.* **3**, 394–405 (2024).
45. Jung, S., Shin, S., Park, S. & Hong, S. Visible-Light-Driven C4-Selective Alkylation of Pyridinium Derivatives with Alkyl Bromides. *J. Am. Chem. Soc.* **142**, 11370–11375 (2020).
46. Lee, W., Jung, S., Kim, M. & Hong, S. Site-Selective Direct C-H Pyridylation of Unactivated Alkanes by Triplet Excited Anthraquinone. *J. Am. Chem. Soc.* **143**, 3003–3012 (2021).
47. Cao, H. *et al.* Brønsted acid-enhanced direct hydrogen atom transfer photocatalysis for selective functionalization of unactivated C(sp³)-H bonds. *Nat. Synth.* **1**, 794–803 (2022).
48. Zhou, M. *et al.* Alkyl sulfonates as cross-coupling partners for programmable and stereospecific installation of C(sp³) bioisosteres. *Nat. Chem.* **15**, 550–559 (2023).
49. Locke, G. M., Bernhard, S. S. R. & Senge, M. O. Nonconjugated Hydrocarbons as Rigid-Linear Motifs: Isosteres for Material Sciences and Bioorganic and Medicinal Chemistry. *Chem. Eur. J.* **25**, 4590–4647 (2019).
50. Mykhailiuk, P. K. Saturated bioisosteres of benzene: where to go next? *Org. Biomol. Chem.* **17**, 2839–2849 (2019).

ACKNOWLEDGEMENTS

This research was supported financially by the Institute for Basic Science (IBS-R010-A2).

AUTHOR INFORMATION

Corresponding Author

*E-mail: hongorg@kaist.ac.kr

ORCID

Sungwoo Hong: 0000-0001-9371-1730

Leejae Kim: 0009-0001-7804-0120

Wooseok Lee: 0000-0003-0982-106X

AUTHOR CONTRIBUTIONS

§L.K. and W.L. contributed equally. L.K., W.L., and S.H. conceptualized the study and wrote the manuscript. L.K. and W.L. conducted the experiments, and W.L. performed the DFT calculations. All authors contributed to data analysis, interpretation of results, and manuscript review.

COMPETING INTERESTS

The authors declare no competing interests.